Military Technical College
Kobry El-Kobba,
Cairo, Egypt

11-th International Conference
on Aerospace Sciences &
Aviation Technology

CALCULATION OF AERODYNAMIC HEATING OF A CONICAL FOREBODY ALONG FLIGHT TRAJECTORY

Ahmed, M. Y. Zayed, A-N. Said, M. K.

ABSTRACT

The phenomenon of aerodynamic heating is created as a consequence of body-flow interaction. It is originated from viscous flow characteristics inside the boundary layer in the vicinity of body. The adjacent flow temperature increases, leading to an increase in body wall temperature depending on flow regime, surrounding air density, body velocity, wall material, flight time, etc.. The present work provides an illustrative calculation procedure based on closed-form relations. A computer program was implemented to be used as a quick, easy, and accurate calculation tool for the expected wall temperature distribution and its variation with flight time for a conical fore-body during a complete flight at zero incidence. The code was applied on a number of real cases with a variety of flight conditions. Results were compared with published and previous work and showed very good agreement.

KEY WORDS: Aerodynamic heating, boundary layer theory, viscous flow

NOMENCLATURES

a	Speed of sound
c_f	Skin friction coefficient
c_p	Specific heat at constant pressure
h	Heat transfer coefficient
i	Enthalpy
kn	Knudsen number
l	Mean free path length
Ln	Nose generation
M	Mach number
Nu	Nusselt number
p, P	Pressure
Pr	Prandtl number
q	Heat transfer rate, dynamic pressure
r	Recovery factor
Re	Reynolds number
St	Stanton number
t	Time
T	Temperature
V	Velocity
β	Angle of inclination, effective Mach
γ	Specific heat ratio
δ	Boundary layer thickness, thickness
ε	Emissivity, nose bluntness
η	Accommodation coefficient
λ	Coefficient of thermal conductivity
$\overline{\lambda}$	Velocity gradient at stagnation point
μ	Dynamic viscosity coefficient
ν	Kinetic viscosity coefficient
ρ	Density
σ	Stephan-Boltzmann constant

Subscripts

inc	Incompressible
l	Mean free path, local
L	Laminar
N	Nose
m	Mean
o	Stagnation, sea level
r	Recovery, radiation
s	Shock wave
T	Turbulent

1. INTRODUCTION

As the missile flies through the atmosphere, it experiences heat transfer from heated gas, adjacent to the wall, to the wall and vice versa as a consequence of flow stagnation inside the boundary layer in the vicinity of the flying body [1,2,3].

Being able to predict the net amount of heat transferred to the missile body during flight has become a vital step in missile design activities, Fig. 1, since almost all modern missiles carry very delicate guidance and control devices and/or carry very sensitive warheads. Controlling the amount of heat transferred to the missile on-board equipment and the maximum allowable temperature in missile interior is obviously of a must.

In the present work, a mathematical model was developed for the estimation of aerodynamic heating over a conical forebody with a zero angle of attack. The mathematical model is based on closed form governing equations that govern the body-flow interaction according to the flow regime. The boundary layer theory governs these relations in the dense atmosphere, while the molecular kinetic theory describes these relations better in cases of high rarefaction or sharp decrease of air density.

A computer code was implemented having the following characteristics:

- Evaluating the drag forces acting on a complete missile body.
- Predicting the trajectory of a medium- to- long range unguided ballistic missile under the assumptions of: point mass body flying in a one plane with zero angle of attack with a constant mean thrust or a thrust –time table in a stagnant air around a fixed circular Earth
- Estimating the aerodynamic heating parameters with time along the complete trajectory. These parametrs are: the net heat flow rate and the temperature profile over a conical forebody.

The code was applied on a number of real missiles and the results were compared with previous works and showed a very good agreement.

2. MATHEMATICAL MODEL

The model being constructed in this study adopts the thin skin (wall) assumption. The conical fore-body, Fig. 2, is divided into a finite number of segments.

The net local value of heat transfer rate is determined according to the appropriate governing theory. This value is used in a heat transfer problem to modify the wall temperature within the time increment previously determined.

The flow regime; continuum, slip, or free molecular flow dictates the governing theory. Obviously, the regime of the flow must be specified first according to the local value of Knudsen number

The local value of Knudsen number is evaluated for both laminar and turbulent flows, respectively as follows [3]:

$$Kn = 0.264\sqrt{\gamma}\,M/\sqrt{Re} \qquad \text{If } Re \le 5e5 \qquad (1)$$

$$Kn = 3.39\sqrt{\gamma}\,M/Re^{4/5} \qquad \text{If } Re > 5e5 \qquad (2)$$

where Re the local value of Reynolds number ($Re = \frac{Vx}{\nu}$), and x is the position of point of calculations from the nose tip, Fig. 2 . If Knudsen value is less than or equal to 0.01 the flow is considered to be in viscous continuum regime, and is said to be in the free molecular flow regime if Knudsen exceeds unity and to fall in the "intermediate" slip flow regime if Knudsen has the values ranging from 0.01 to unity.

2.1. Aerodynamic Heating in Continuum Flow Regime

- **Non-viscous (edge) properties**

The non-viscous flow properties at the edge of the boundary layer are evaluated relative to the free stream values as follows [2]:

$$\frac{T_\delta}{T_\infty} = \left(1 - \tilde{v}_c^{\,2}\right)\left(1 + \frac{\gamma - 1}{2} M_\infty^2\right) \qquad (3)$$

$\tilde{v}_c = \frac{V_\delta}{V_{max}}$ is the ratio between the velocity downstream of the shock wave and a certain hypothetical velocity $V_{max} = \sqrt{2\gamma(p_o/\rho_o)/(\gamma - 1)}$ with p_o and ρ_o are the stagnation pressure and density of the flow behind the shock wave. The value $\tilde{v}_c$ is given in charts as a function of free stream Mach number and the cone semi apex angle [2].

$$\frac{p_\delta}{p_\infty} = v_o \left(\frac{T_\delta}{T_\infty}\right)^{\gamma/(\gamma-1)} \qquad (4)$$

with $v_o = \dfrac{1}{\left[(1+\varepsilon)K_o^2 - \varepsilon\right]^{(1-\varepsilon)/2\varepsilon}\left(\varepsilon + \dfrac{1-\varepsilon}{K_o^2}\right)^{(1+\varepsilon)/2\varepsilon}}$

where $\varepsilon = (\gamma - 1)/(\gamma + 1)$ and $K_o = M_\infty \sin\theta_s$, with θ_s is the angle that the shock wave makes with the free stream flow direction. The value of K_o depends on the value of $K_1 = M_\infty \delta_c$ according to the following rule,

$$K_o = \left(1 + \frac{\gamma_\infty + 1}{2} K_1^2\right)^{1/2} \qquad \text{if } K_1 \le 6$$

$$K_o = \left[0.39 - 0.01\log\left(\frac{p_\infty}{p_{SL}}\right)\right] + \left[1.03 + 0.005\log\left(\frac{p_\infty}{p_{SL}}\right)\right] K_1 \qquad \text{if } K_1 > 6$$

where p_{SL} is the value of atmospheric pressure at sea level conditions.

$$\frac{\rho_\delta}{\rho_\infty} = \frac{p_\delta / p_\infty}{T_\delta / T_\infty} \qquad (5)$$

$$\frac{c_{p_\delta}}{c_{p_\infty}} = \left(\frac{T_\delta}{T_\infty}\right)^{0.1} \qquad (6)$$

$$\frac{\mu_\delta}{\mu_\infty} = \left(\frac{T_\delta}{T_\infty}\right)^{0.7} \quad (7) \qquad \frac{a_\delta}{a_\infty} = \sqrt{\frac{T_\delta}{T_\infty}} \quad (8)$$

$$M_\delta = \sqrt{\frac{(\gamma-1)}{2}\left(\frac{1}{1-\tilde{v}_c^2}-1\right)} \quad (9) \qquad \frac{V_\delta}{V_\infty} = \frac{M_\delta}{M_\infty}\frac{a_\delta}{a_\infty} \quad (10)$$

- **Boundary layer properties**

The wall enthalpy i_w; at each point is then evaluated as a function of temperature and pressure [2].

The flow parameters inside the boundary layer may be calculated considering compressibility of gas and ignoring influence of temperature rise or considering the temperature rise and ignoring compressibility [2]. The decision to choose either way depends mainly upon the value of Mach number of the free stream. The "switching" Mach number was found to have the value of 5.2 [5]. The viscous flow properties in each case are evaluated as follows.

Case1: temperature rise is more significant

The effective flow parameters are evaluated as follows:

$$i^* = 0.5(i_w + i_\delta) + 0.22(i_r - i_\delta) \quad (11)$$

here i_w, i_δ, and i_r are the wall, edge, and recovery enthalpies, respectively. where

$$i_r - i_\delta = r\frac{V_\delta^2}{2} \quad (12)$$

r is the recovery factor

$$r = (Pr)^a \quad (13)$$

where a = 0.5 for laminar flow and a = 1/3 for turbulent flow. For calculation purposes, Prandtl number equals 0.71 for air at normal temperature [3].

$$i_\delta = c_{p_\delta} T_\delta \quad (14)$$

T^*; is evaluated from effective enthalpy, figure 4.

$$\frac{\rho^*}{\rho_\delta} = \frac{T_\delta}{T^*} \quad (15) \qquad \frac{c_p^*}{c_{p_\delta}} = \left(\frac{T^*}{T_\delta}\right)^{0.1} \quad (16)$$

$$\frac{\mu^*}{\mu_\delta} = \left(\frac{T^*}{T_\delta}\right)^{0.7} \quad (17) \qquad \frac{\lambda^*}{\lambda_\delta} = \left(\frac{T^*}{T_\delta}\right)^{0.85} \quad (18)$$

$$\frac{\lambda^*}{\lambda_\delta} = \left(\frac{T^*}{T_\delta}\right)^{0.85} \quad (19) \qquad Re^* = Re_\delta \left(\frac{\rho^*}{\rho_\delta}\right) \Big/ \left(\frac{\mu^*}{\mu_\delta}\right) \quad (20)$$

The local skin friction drag coefficient

$$c_{f_x}^{\cdot} = C \times D \times \left(Re_x^{\cdot}\right)^n \tag{21}$$

The values of C , D , and n have different values according to table 1.

Table 1. Coefficients used to calculate Reynold's number

Parameter	Laminar flow	Turbulent flow
C	$\sqrt{3}$	1.17
D	0.664	0.0578
N	$-1/2$	$-1/5$

Local Stanton number; $$St_x^{\cdot} = \frac{1}{2} c_{f_x}^{\cdot} \left(Pr^{\cdot}\right)^{-\frac{2}{3}} \tag{22}$$

The heat transfer coefficient; at each point is evaluated from the relation

$$h_x^{\cdot} = St_x^{\cdot} c_p^{\cdot} \rho^{\cdot} V_{\delta} \tag{23}$$

Finally ***the heat transfer rate*** at any point on the cone generator can be calculated from the relation

$$q_o = h_x^{\cdot} \frac{\left(i_r - i_w\right)}{c_{p_m}} \tag{24}$$

where c_{p_m} is the mean value of specific heats calculated at the recovery and wall temperatures.

Case2: compressibility is more significant

The local skin friction drag coefficient; for laminar and turbulent flow cases, respectively, is

$$\frac{c_{fL}}{c_{fL}^0} = \left(1 + 0.03 M_{\infty}^2\right)^{-\frac{1}{3}} \tag{25}$$

$$\frac{c_{fT}}{c_{fT}^0} = \left(1 + 0.12 M_{\infty}^2\right)^{-\frac{1}{2}} \tag{26}$$

where c_{fT}^0 is the incompressible skin friction drag coefficient which can be calculated through equation 21 and table 1.

Local Stanton number; $$St_x = \frac{1}{2} c_{f_x} \left(Pr\right)^{-\frac{2}{3}} \tag{27}$$

The heat transfer coefficient; $$h_x = St_x c_p \rho V_{\delta} \tag{28}$$

Finally ***the heat transfer rate*** at any point on the cone generator can be calculated from the relation

$$q_o = h_x \frac{\left(i_r - i_w\right)}{c_{p_m}} \tag{29}$$

where the recovery enthalpy i_r is evaluated as $i_r = (i_r - i_\delta) + i_\delta$. Again, the enthalpy difference $(i_r - i_\delta)$ and i_δ are given in Eqs. (12) and (14), respectively, and c_{p_m} is the mean value of specific heats calculated at the recovery and wall temperatures.

2.2. Aerodynamic Heating in Slip Flow Regime

Being intermediate regime, the calculations of the heat transfer during the slip flow regime are constructed based upon those of the continuum flow regime. The local heat transfer rate in this regime at any point is evaluated in the following manner.

The length of the mean free path l; at any point is evaluated by

$$l = 1.255\nu\frac{\sqrt{\gamma}}{a} \tag{30}$$

where γ is the specific heat ratio, ν is kinetic viscosity and "a" is the speed of sound of the flow.

Heat transfer rate q; is evaluated by the relation [2]

$$q_o = q^c\left(1 - \frac{1.89}{\bar{\chi}} + \frac{10.7}{\bar{\chi}^2}\right) \tag{31}$$

with q^c is the local heat transfer rate evaluated as if the flow were in the continuum regime, and

$$\bar{\chi} = \frac{2.89\bar{x}}{Re_l} \tag{32}$$

with $\bar{x} = \frac{x}{l}$, where x is the local distance from nose apex and Re_l is the local value of Reynolds number based on the free length l.

2.3. Aerodynamic Heating in Free Molecular Flow Regime

According to the molecular kinetic theory, the local heat transfer rate is given by [3]

$$q_o = \eta\rho_i\sqrt{\frac{(RT_i)^3}{2\pi}}\left\{\left[e^{-\bar{x}^2} + \bar{x}\sqrt{\pi}(1+\mathrm{erf}(\bar{x}))\right]\left[\bar{x}_\infty^2 - \frac{\gamma+1}{2(\gamma-1)}\cdot\frac{T_w}{T_i} + \frac{\gamma+1}{2(\gamma-1)}\right] + \frac{1}{2}\bar{x}\sqrt{\pi}(1+\mathrm{erf}(\bar{x}))\right\} \tag{33}$$

where ρ_i and T_i are the density and temperature of the incident molecules (atmospheric values), η is the accommodation coefficient and it ranges from 0.7 to 0.97 [1] (an average value of 0.85 is assumed), T_w is the local wall temperature and the error function

$$\mathrm{erf}(x) = \frac{2}{\sqrt{\pi}}\int_0^x e^{-z^2}dz \tag{34}$$

and

$$\bar{x} = M_\infty\sqrt{\gamma/2}\sin(\beta) = \bar{x}_\infty\sin(\beta) \tag{35}$$

with β the inclination angle of surface to flow direction (here it is taken to be equal to the nose semi-apex angle).

2.4. Aerodynamic Heating at the Stagnation Point

Recovery enthalpy of the flow i_r; $$i_r = i_\infty + \frac{V_\infty^2}{2} \quad (36)$$

Free stream stagnation temperature T_{o1} [6]; $$T_{o1} = T_\infty\left(1+\frac{\gamma-1}{2}M_\infty^2\right) \quad (37)$$

Free stream stagnation pressure P_{o1} [6]; $$P_{o1} = P_\infty\left(1+\frac{\gamma-1}{2}M_\infty^2\right)^{\frac{\gamma}{\gamma-1}} \quad (38)$$

Free stream stagnation density ρ_{o1} [6]; $$\rho_{o1} = \rho_\infty\left(1+\frac{\gamma-1}{2}M_\infty^2\right)^{\frac{1}{\gamma-1}} \quad (39)$$

Stagnation temperature behind the normal shock wave T_{o2}; under the assumption of adiabatic flow through a normal shock wave [6]; hence, $T_{o2} = T_{o1}$

Stagnation pressure behind the normal shock wave P_{o2}; [1]

$$P_{o2} = \frac{P_{o1}}{\left[(1+\varepsilon)M_\infty^2 - \varepsilon\right]^{\frac{1-\varepsilon}{2\varepsilon}}\left(\varepsilon+\frac{1-\varepsilon}{M_\infty^2}\right)^{\frac{1+\varepsilon}{2\varepsilon}}} \quad (40)$$

where $\varepsilon = \frac{\gamma-1}{\gamma+1}$

Stagnation density behind the normal shock wave ρ_{o2}; $$\frac{\rho_{o2}}{\rho_{o1}} = \frac{P_{o2}}{P_{o1}} \quad (41)$$

Velocity gradient at the stagnation point; $$\tilde{\lambda} = \bar{\lambda}\frac{V_\infty}{D_N} \quad (42)$$

where D_N is the diameter of the nose tip, V_∞ is the free stream velocity. The dimensionless velocity gradient $\bar{\lambda}$ is given as a function of flight Mach number [2].

Density ratio; $\bar{\rho}_w = \frac{\rho_w}{\rho_{o2}}$ for $M_\infty \geq 1$, and $\bar{\rho}_w = \frac{\rho_w}{\rho_{o1}}$ for $M_\infty < 1$

Viscosity ratio; $\bar{\mu}_w = \frac{\mu_w}{\mu_{o2}}$ for $M_\infty \geq 1$, and $\bar{\mu}_w = \frac{\mu_w}{\mu_{o1}}$ for $M_\infty < 1$

Heat transfer rate to the wall [2];

$$q_o = \frac{0.763}{Pr^{2/3}}\sqrt{\tilde{\lambda}\rho_{o2}\mu_{o2}}(i_r - i_w)(\bar{\rho}_w\bar{\mu}_w)^{0.1} \quad \text{for } M_\infty \geq 1 \quad (43)$$

$$q_o = \frac{0.763}{Pr^{2/3}} \sqrt{\tilde{\lambda}\rho_{o1}\mu_{o1}} (i_r - i_w)(\bar{\rho}_w \bar{\mu}_w)^{0.1} \qquad \text{for } M_\infty < 1 \qquad (44)$$

The radiation heat transfer can be calculated at each point simply adopting the well-known Stefan-Boltzmann law

$$q_r = \varepsilon \sigma T_w^4 \qquad (45)$$

where ε : the wall emissivity and
σ : Stefan-Boltzmann coefficient [5.6697×10^{-8} $W/(m^2.K^4)$].

The neat heat flux to the wall is readily evaluated as

$$q_w = q_o - q_r \qquad (46)$$

2.5. Wall Temperature

The change 0in a thin wall temperature due to heat flux equals

$$\Delta T_w = \frac{q_w . \Delta t}{c.\rho.\delta} \qquad (47)$$

where q_w is the net heat flux to the wall in [W/m^2], Δt is the time increment of exposure, c , ρ , and δ are the specific heat, density, and thickness of wall material. The wall temperature at any instant is

$$T_w = (t + \Delta t) = T_w(t) + \Delta T_w \qquad (48)$$

3. CASE STUDIES

The implemented program was applied to a number of real rockets with a variety of flight conditions such as, flight time from 80 to 600 seconds, ranges from 20 to 1800 km, apogee from 8 to 300 km, maximum Mach number from 2 to 16. Sample results are illustrated in Figs. 3-11.

- **Missile1:**

An unguided, single solid stage, fin-stabilized ground-to-ground rocket

– Mean thrust	21225	N
– Launching mass	64.525	Kg
– Propellant mass	19.0	Kg
– Burning time	1.74	s
– Maximum range	20.4	Km
– Corresponding altitude	7.8	Km
– Maximum Mach number	2.4	

The output, of running these data on the implemented program, is presented in Fig. 3 which displays the wall temperature at three different locations on the missile nose during the flight time. Figure 4 displays the variation with time of flight parameters and wall temperature at 0.1 nose generator length.

• **Missile 2:**

A tactical unguided rocket fired from an oblique launcher.

– Mean thrust	346565	N
– Launching mass	2450	Kg
– Propellant mass	1143	Kg
– Burning time	9.53	sec
– Maximum range	75	Km
– Corresponding altitude	20	Km
– Maximum Mach number	4.8	

• **Missile 3:**

A long range, single stage, liquid propelled ballistic missile. A typical flight of this missile consists mainly of a short vertical rise path, a gravity turn path, a constant attitude path, and a passive part.

– Mean thrust	133000	N
– Launching mass	5686.5	Kg
– Propellant mass	3612.5	Kg
– Burning time	59.0	s
– Maximum range	300	Km
– Corresponding altitude	89	Km
– Maximum Mach number	5.3	

• **Missile 4:**

This missile is a single stage, unguided ballistic missile. It is required to deliver a payload of at least 200 Kg to an apogee of about 300 Km.

– Mean thrust	238674	N
– Launching mass	4043.6	Kg
– Propellant mass	2900	Kg
– Burning time	36	s
– Maximum range	147	Km
– Corresponding altitude	312	Km
– Maximum Mach number	8	

• **Missile 5:**

An intermediate-range, two-stage, solid propelled, hypersonic ballistic missile.

– Mean thrust	109500	N
– Launching mass	7200	Kg
– Propellant mass	5838	Kg
– Burning time	105	s
– Maximum range	1800	Km
– Corresponding altitude	300	Km
– Maximum Mach number	16	

Figures 5-11 show the obtained skin temperatures of the missiles 2-5 and variation of flight parameters respectively during the flight times.

4. VERIFICATION OF RESULTS

A comparison between results of the implemented program and previous work [4] for sample missile 4 is shown in Fig. 12. The results show a sufficient agreement with previous work, the difference gives an error of about 4%.

5. CONCLUSIONS

A computer code was developed in this work so as to facilitate the estimation of aerodynamic heating phenomena. The code can also be used in estimating the complete trajectory and missile drag components as functions of Reynold and Mach numbers. The code results showed good agreement with previous works. Some important conclusions could be deduced through analyzing the case study results:

- The heat transfer rate has a maximum value exactly at the nose tip.
- As the nose bluntness increases, the nose tip temperature decreases continuously for the sane flight parameters.
- As the nose vertex angle increases, the wall temperature increases for the same flight parameters.
- Isolating the effect of altitude variation, the wall temperature follows approximately the behavior of flight velocity. The rate of change of wall temperature approximately behaves like acceleration. If the missile is flying with a positive acceleration, the wall temperature increases with a certain rate, if this positive acceleration decreases in magnitude, the wall temperature increases with a lower rate. The opposite is also true.
- At the moment of reentry, altitudes of about 75- 80 km, the missile experiences a severe heat transfer reaching very high rates.
- The event of maximum wall temperature is most likely to happen during atmospheric flight.

REFERENCES

[1] N.F.Krasnov, "Aerodynamics", Amerind Publishing, New Delhi 1978.
[2] N.F.Krasnov, "Aerodynamics of Bodies of Revolution", second edition, Elsevier, New York 1970.
[3] James R.Hayes and Richard D. Neumann, "Introduction to Aerodynamic Heating Analysis of Supersonic Missiles", "Tactical Missile Aerodynamics: Prediction Methodology", AIAA Tactical Missile Series, Volume 142, ISBN 1-56347-016-0, 1991.
[4] Classified publication.
[5] Dubin. M. et al., U. S. Standard Atmosphere 1962, U. S. Government Printing Office, Washington, D. C., 1962.
[6] John D. Anderson, "Fundamentals of Aerodynamics", second edition, McGraw-Hill International Editions, Aerospace Science Series, ISBN 0-07-100767-9, 1991.
[7] A. R. El-Ashmawi, "Drag Prediction Methodology for Missiles at Subsonic, Transonic, and Supersonic Speeds", M. Sc. Thesis, Military Technical college, Cairo, Egypt, 1983.
[8] A. H. Helmy and H. Hosny, "Re-entry Performance", Diplom course, Military Technical College, Cairo, Egypt, 1979.
[9] Heinz Schulte, "Pershing II", international defence review magazine,1983.

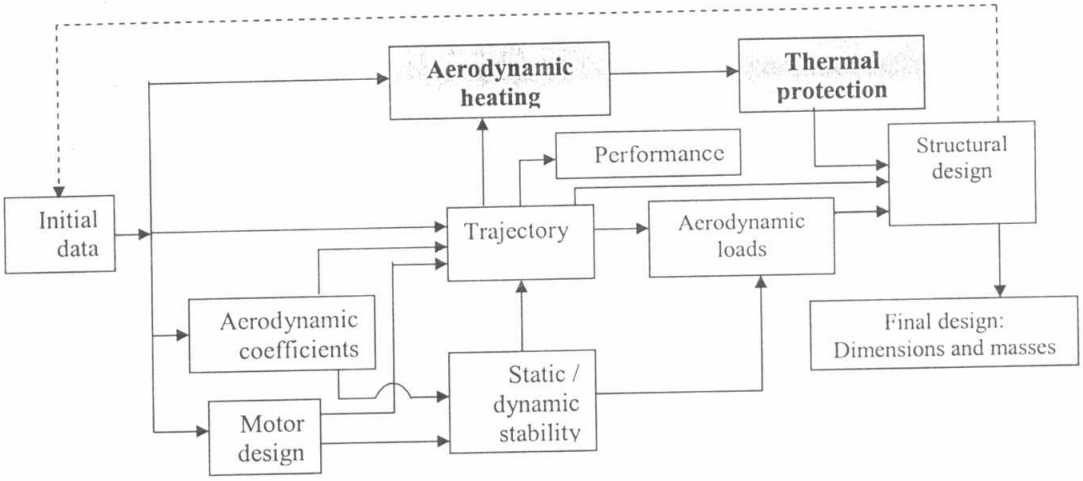

Fig. 1 Scheme illustrating the Missile System Analysis

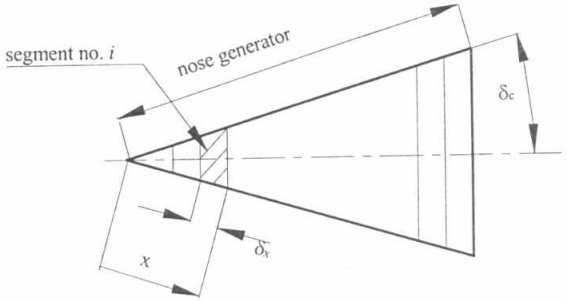

Fig. 2 Segmentation of the nose

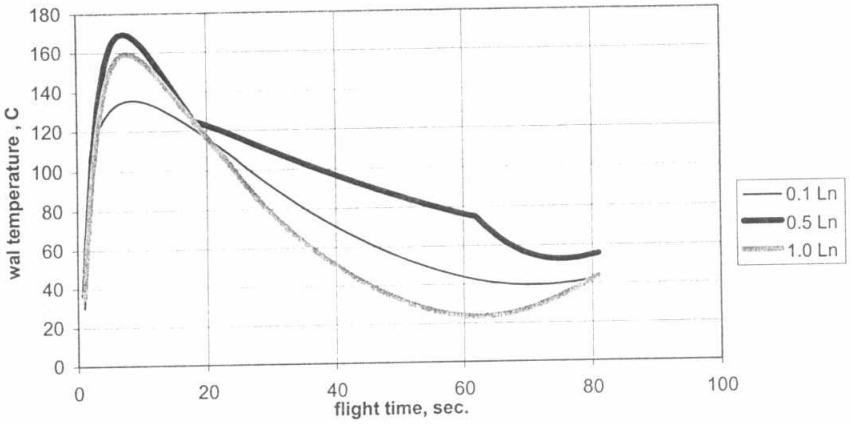

Fig.3 Variation of wall temperature with flight time of missile "1", vertex angle = 9°

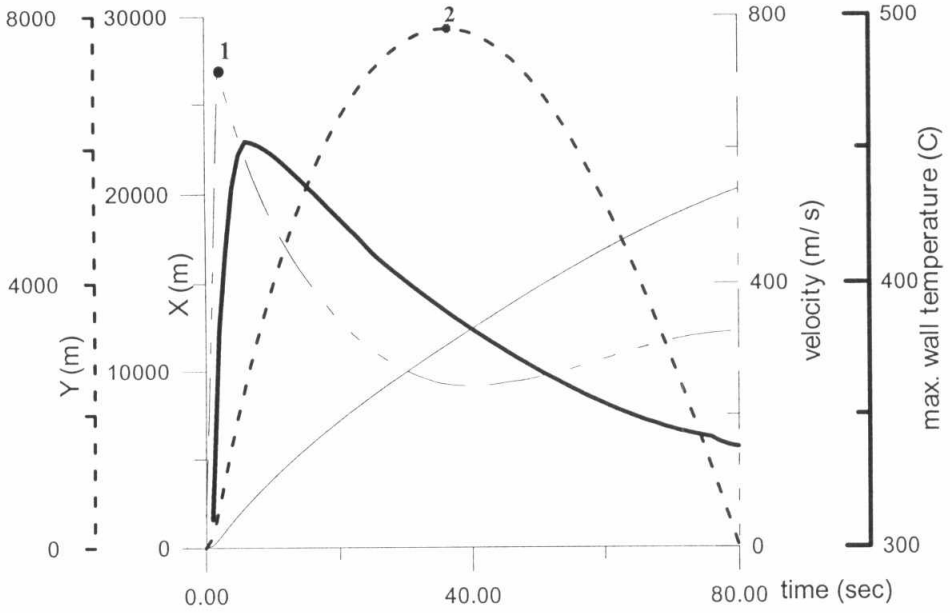

Fig. 4 Variation of flight parameters with flight time of missile "1"

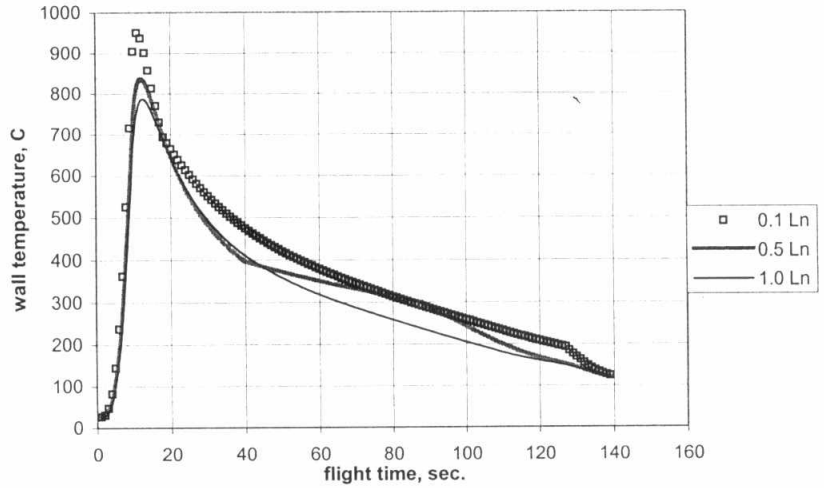

Fig.5 Variation of wall temperature with flight time of missile "2", vertex angle =13 °

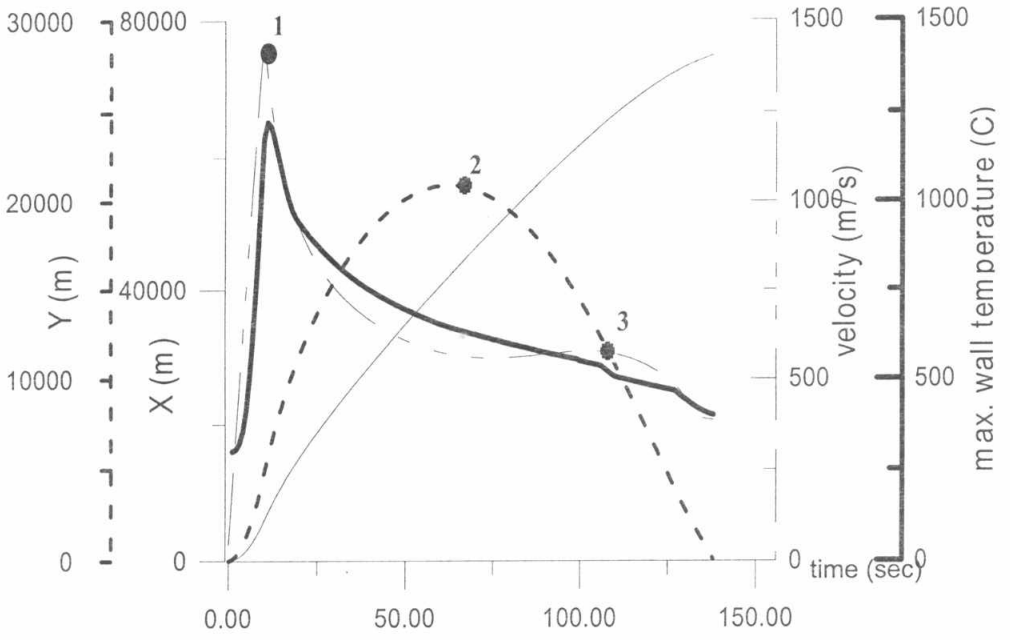

Fig. 5 Variation of flight parameters with flight time of missile "2"

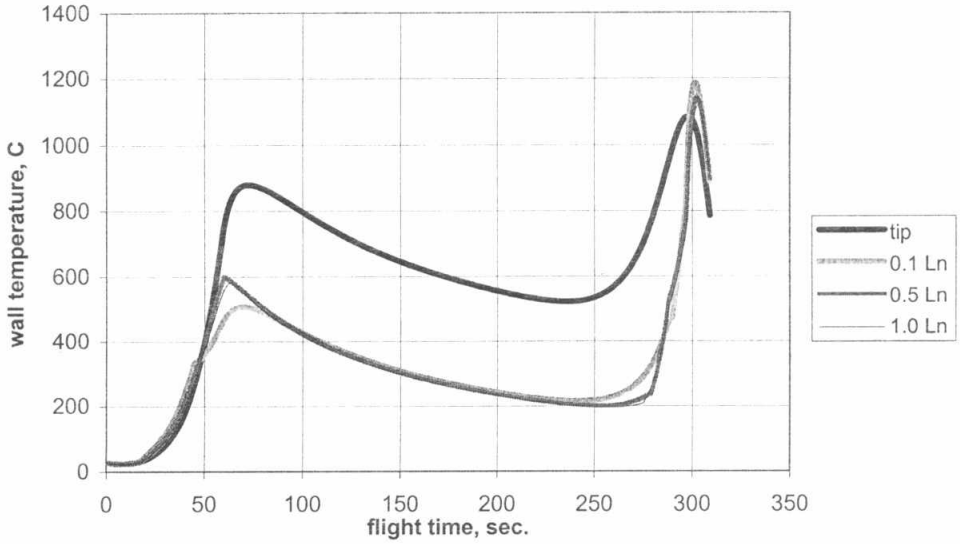

Fig.6 Variation of wall temperature with flight time of missile "3", vertex angle = 11 °

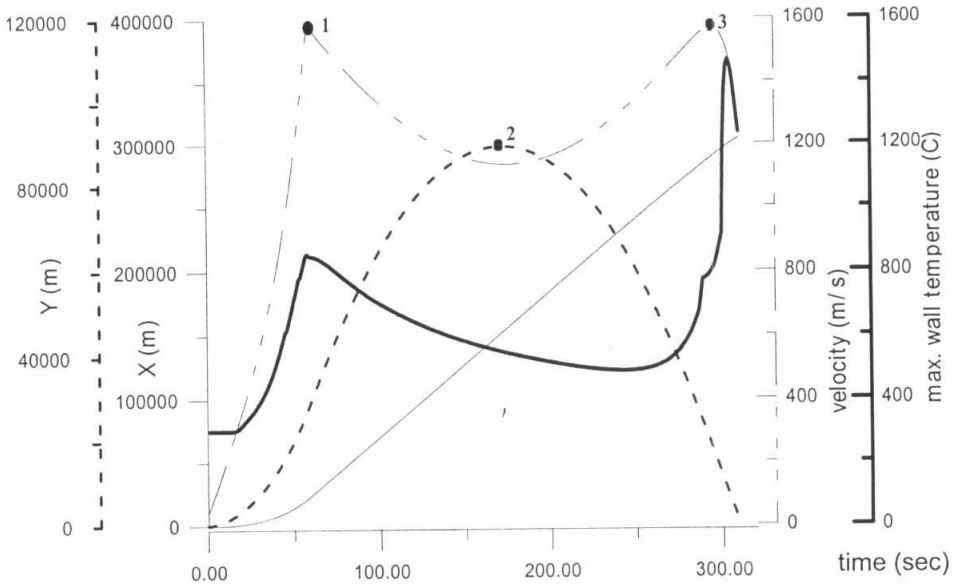

Fig. 7 Variation of flight parameters with flight time of missile "3"

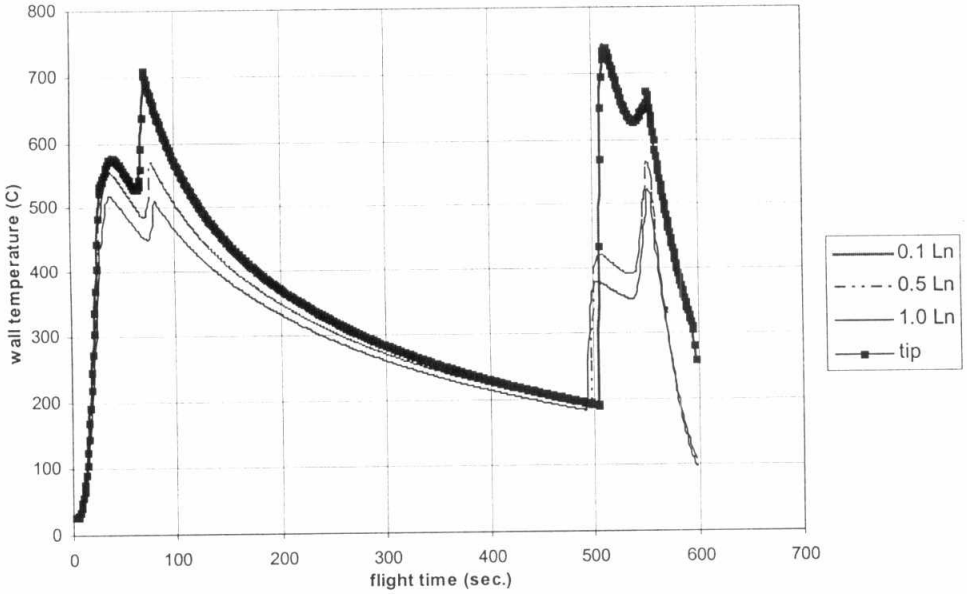

Fig.8 Variation of wall temperature with flight time of missile "4", vertex angle = 11.3 °

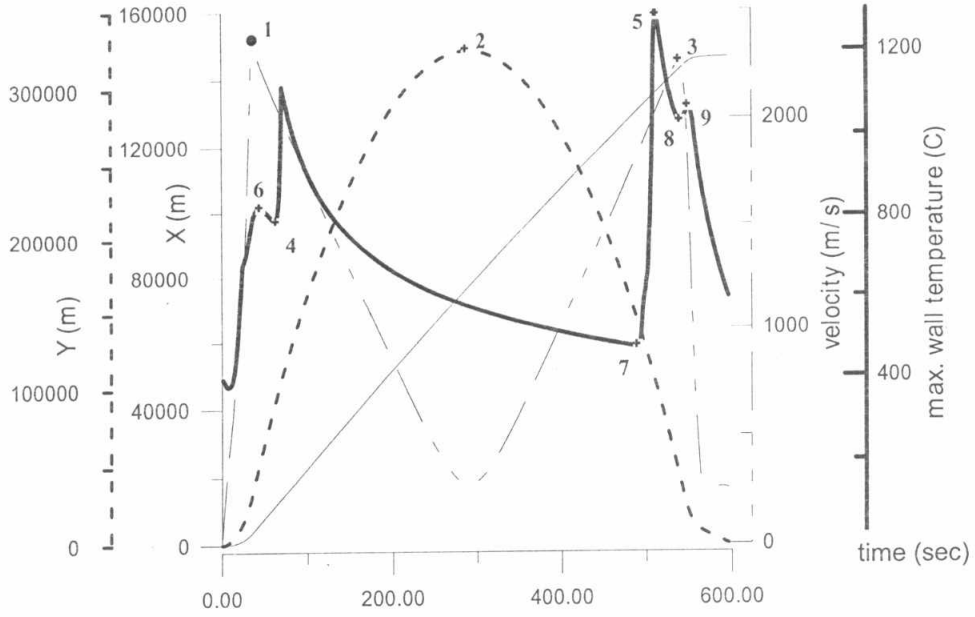

Fig. 9 Variation of flight parameters with flight time of missile "4"

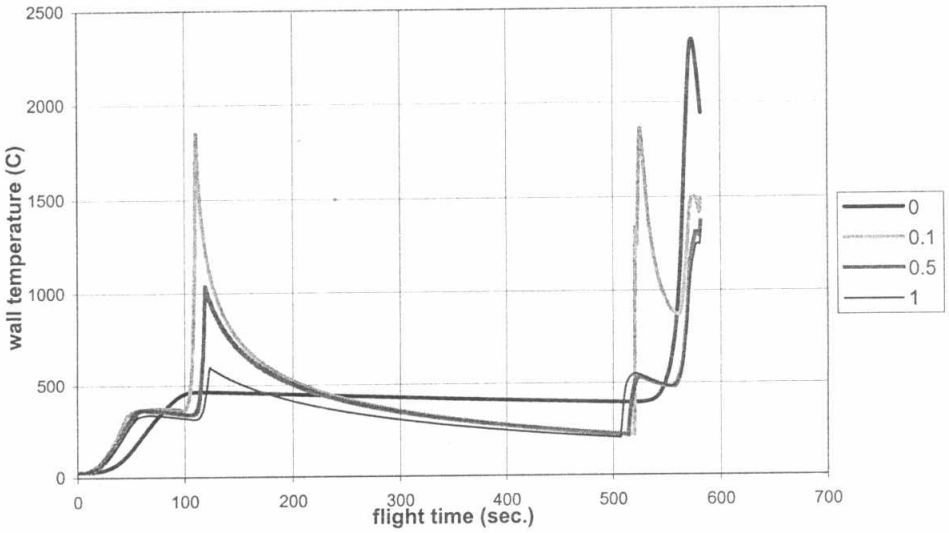

Fig.10 Variation of wall temperature with flight time of missile "5", vertex angle = 7 °

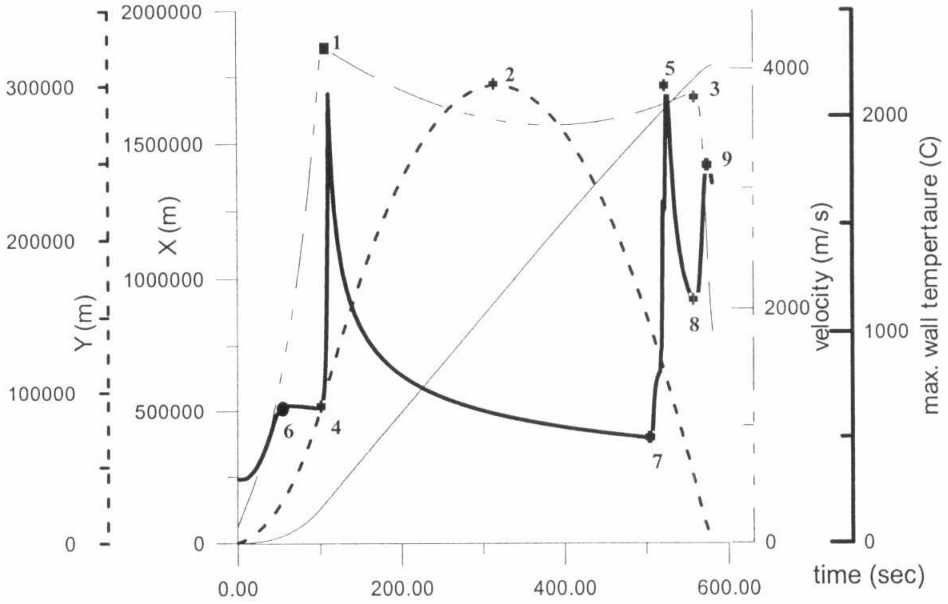

Fig. 11 Variation of flight parameters with flight time of missile "5"

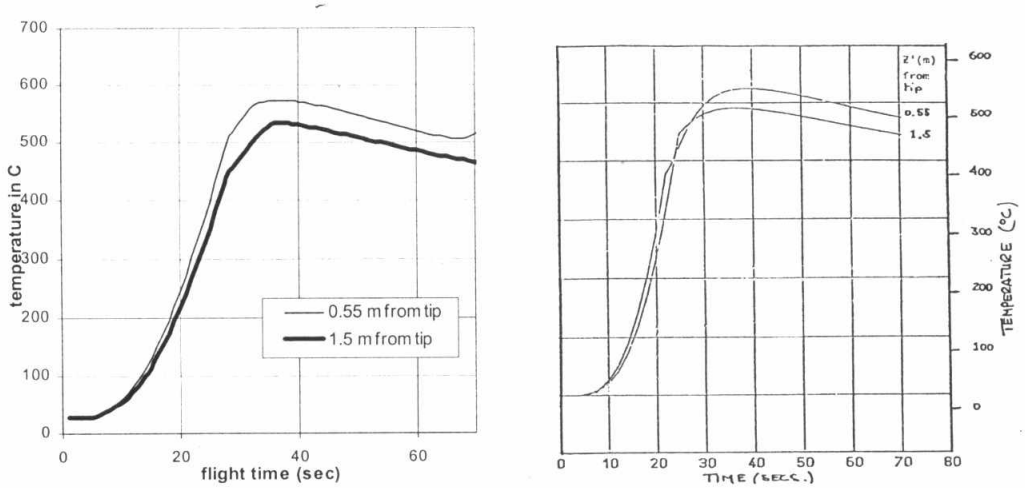

(a) (b)

Fig.12 Comparison between (a) results obtained from the code and (b) data presented in previous work [4]